Density Functional Theory Study of NO Adsorbed in A-Zeolite

Ya-Jun Liu,[†] Anders Lund,[‡] Petter Persson,[†,§] and Sten Lunell*[,†]

Department of Quantum Chemistry, Uppsala University, Box 518, S-751 20 Uppsala, Sweden, Chemical Physics Laboratory, IFM Linköping University, S-581 83 Linköping, Sweden, and Materials and Process Simulation Center, Beckman Institute 13974, California Institute of Technology, Pasadena, California 91125

Received: December 21, 2004; In Final Form: February 24, 2005

Density functional theory was employed to investigate the adsorption site and hyperfine interactions of nitric oxide adsorbed in Na-LTA (previous name NaA) zeolite. Three different cluster models of increasing complexity were used to represent the zeolite network: (1) a six-membered ring terminated by hydrogen atoms with one sodium ion above the ring, (2) as model 1 with the addition of three sodium ions located at the centers of three imagined four-membered rings adjacent to the six-membered ring, and (3) as model 2 with the addition of the three four-membered rings adjacent to the six-membered ring. Calculations on the largest system (model 3) showed very good agreement with measured electronic Zeeman interaction couplings, ^{14}N hyperfine coupling tensors, and ^{23}Na hyperfine and nuclear quadruple coupling tensors of the $S = {}^1/_2$ $Na^+\cdots N-O$ adsorption complex when the position of the sodium ion was relaxed. The optimized geometry of the complex agreed nicely with that estimated experimentally, except for the Na−N distance, where the present results indicate that the distance deduced from previous ENDOR experiments may be underestimated by as much as 0.5 Å.

I. Introduction

Nitric oxide, NO, has been recognized as an atmospheric pollutant and a potential health hazard. Methods for NO removal from exhaust streams, such as catalytic decomposition and selective catalytic reduction with reducing agents, are therefore current topics in the field of environmental protection. In particular, copper ion-exchanged zeolites were found to be most active for such a reaction.[1,2] However, some controversies still remain concerning the reaction mechanism. Studies of NO adsorption are consequently of interest to elucidate the mechanism of catalytic reactions.

The adsorption complexes with odd-electron nitric oxide are usually paramagnetic although ground-state NO in the gas phase is diamagnetic. Adsorption of NO on zeolites has consequently been studied for more than three decades applying electronic paramagnetic resonance (EPR) for the characterization of adsorption and desorption behavior. Lunsford[3] was the first to report the EPR spectra of NO adsorbed on Na-FAU(Y) and NH_4-FAU(Y) zeolites. A number of EPR studies of NO adsorbed on zeolites have since been reported, but in several cases the EPR spectra were very ill-resolved, preventing detailed analysis.[4] Kasai and Bishop[5] noticed, however, that the spectra for NO adsorbed on certain zeolites became sharper after keeping the samples at room temperature for several days and demonstrated that the triplet hyperfine interaction with the ^{14}N nucleus ($I = 1$) is clearly resolved at the *y*-component. These earlier EPR studies of the NO/zeolite system have been reviewed.[6] Also, a large number of EPR studies of NO adsorbed on oxides such as MgO, CoO-MgO, ZnO, ZnS, and TiO_2 have been carried out at an early stage and a comprehensive review of the NO/oxide systems was published in 1990.[7] The bonding of NO to zeolites has more recently been investigated by high-resolution methods such as pulsed electronic-nuclear double resonance (ENDOR) and high field EPR to clarify the structure of the active sites where the reduction of NO to harmless products may occur. The adsorption of NO at sodium ions in the Na-LTA zeolite was studied as a model system by Pöppl and co-workers.[8−11] Thus, the local structure of an adsorption complex between sodium ions and nitric oxide was obtained by using pulsed ENDOR. Bond lengths as well as the bond angle of the complex $Na^+\cdots N-O$ were estimated.[10] Their geometric model is shown in Figure 1.

Due to the complexity of the NO/zeolite system, accurate theoretical studies have only recently started to appear in the literature.[12−14] In the present work, we report a detailed analysis of the system that was experimentally characterized by Pöppl and co-workers.[8−11] This has involved the construction of several different models of the Na-LTA zeolite framework, optimization of the geometry of the NaNO part in the zeolite by density functional theory (DFT),[15−16] as well as calculations of isotropic (*a*) and anisotropic (*B*) hyperfine couplings of the ^{14}N and ^{23}Na atoms, quadrupolar couplings (*Q* tensors) of ^{23}Na, and electronic Zeeman interaction couplings (*g* tensors), which are compared with the experimental values. The agreement between calculated and experimental spectral parameters was very satisfacory, indicating the possibility of modeling other similar systems, such as the dimeric complex of nitric oxide, previously observed by EPR to be a triplet state molecule[5,17] and by pulsed EPR[18] to interact with one or more sodium ions in Na-LTA zeolite.

II. Methodology and Basis Sets

DFT calculations utilizing Becke's three-parameter exchange functional[19] with the nonlocal correlation of Lee−Yang−Parr[20] (B3LYP) in Gaussian 03[21] were used to optimize the geometry and calculate isotropic and anisotropic hyperfine coupling constants, using 6-31G(d) and 6-31+G(d) basis sets.[22,23] The

* Corresponding author. E-mail: Sten.Lunell@kvac.uu.se.
[†] Uppsala University.
[‡] Linköping University.
[§] California Institute of Technology.

10.1021/jp044198b CCC: $30.25
Published on Web 03/25/2005

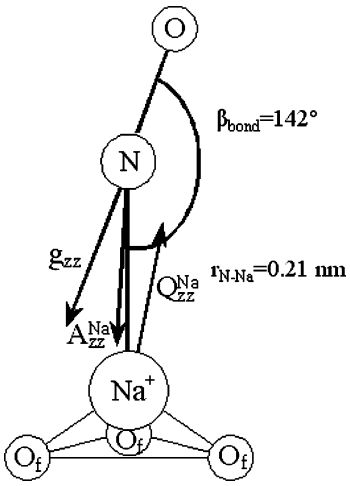

Figure 1. Schematic drawing of the bent structure of the Na^+-NO adsorption complex in Na-LTA zeolite. The Na^+ cation is coordinated to the framework oxygens, O_f, in the six-membered rings (only three oxygens in the first coordination sphere are shown) in a trigonal symmetry (S2 site). More details are given in ref 10.

DFT method with generalized gradient approximation[24] (GGA) Becke[25] and Perdew[26] exchange and correlation functions, and a DZP basis set[27] with relativistic scalar zero order regular approximation[28] (ZORA) core potentials was used in the *g* and *Q* tensor calculations, for which the ADF program was used.[29]

III. Models of Zeolite Framework

The Na-LTA zeolite has a fixed Si/Al = 1 ratio with the chemical formula $Na_{96}(H_2O)_{216}$ $[Si_{96}Al_{96}O_{384}]$ for the hydrated material. For the computations, three models were constructed on the basis of the full cell crystallographic structure of dehydrated zeolite A by Pluth and Smith.[30] They are described as follows.

(A) Model 1. In this model, one six-membered ring is terminated by hydrogen atoms, with each of the H atoms located at a distance of 1.0 Å from the corresponding oxygen atom, and with the O−H bond oriented in the direction of the bond to the next Si or Al atom. A sodium ion is located above the center of the ring, which is at the center of the $O_3-O_3-O_3$ triangle. There are three kinds of O atoms in the A-zeolite, O_3 indicates the third kind of O atom; see ref 30 for details. To keep the complex neutral, two of the Al atoms in the ring were changed to Si, so its molecular formula is $AlSi_5O_6(OH)_{12}Na$ (see Figure 2).

(B) Model 2. In this model, three Na atoms are added to model 1. The Na ions are located at the centers of the three four-membered rings next to the six-membered ring, respectively. To balance the charges of the system to zero, three Si atoms in the ring of model 1 were changed to Al atoms, so its molecular formula is $Al_4Si_2O_6(OH)_{12}Na_4$ (see Figure 3).

(C) Model 3. This model contains one six-membered ring and three four-membered rings adjacent to it, which are terminated by hydrogen atoms. Each of the H atoms is located at a distance of 1.0 Å from the corresponding oxygen atom, and is oriented in the direction of the bond to the next Si or Al atom. Two Al atoms in the central ring were changed to Si atoms for the same reason as in model 1, so its molecular formula is $Al_4Si_8O_{15}(OH)_{18}Na_4$ (see Figure 4).

IV. Results and Discussion

A. Location of the Na Site in Model 1. Each of our models is terminated by H atoms instead of Si and Al atoms as it is in the real zeolite. So, it is unavoidable to get a charged system. To balance the charges, we exchange one or several Si atoms by Al atoms, or vice versa. Here, by optimizing model 1 we attempted to prove that this exchange is reasonable and does not change the zeolite framework too much. We only relaxed the Na atom in model 1 and optimized this model by using B3LYP/6-31G(d), obtaining the calculated results in Table 1. The calculated distance between Na and the center of the six-membered ring, *R*(Na−X), is 0.21 Å, which is identical with

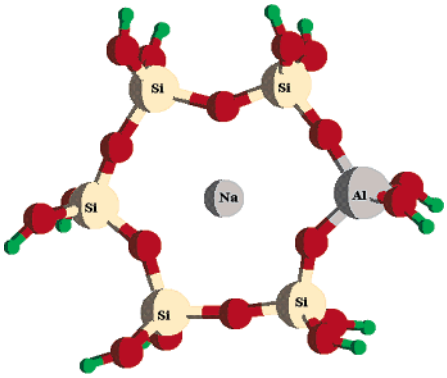

Figure 2. Model 1: One six-membered ring terminated by hydrogen atoms, where each of the H atoms is located at a distance of 1.0 Å from the corresponding oxygen atom, and is oriented in the direction of the bond to the next Si or Al atom. Two Al atoms were in model 1 changed to Si atoms.

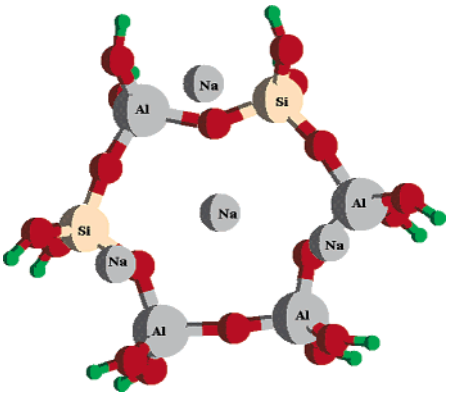

Figure 3. Model 2: Three Na atoms are added to model 1, located at the centers of the three four-membered rings neighboring the six-membered ring, respectively. Three Si atoms in model 1 were changed to Al atoms to preserve electrical neutrality.

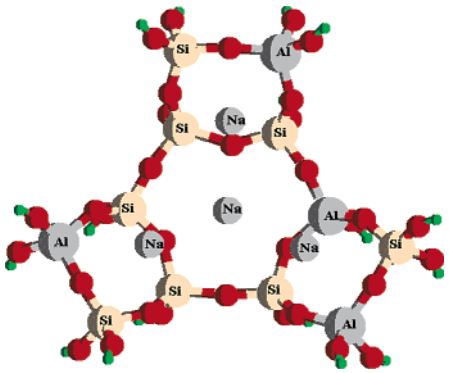

Figure 4. Model 3: One six-membered ring and three four-membered rings connected to it, which are terminated by hydrogen atoms, where each of the H atoms is located at a distance of 1.0 Å from the corresponding oxygen atom, and is oriented in the direction of the bond to the next Si or Al atom. The system contains four Al atoms to charge compensate for the four Na atoms.

TABLE 1: Calculated and Experimental Distances (Å) of Model 1

	R(Na−X)	R(Na−O_2)	R(Na−O_3)	R(Na−Al)	R(Na−Si)
B3LYP[a]	0.210	2.915	2.323	3.264	3.225
BP86[b]	0.740	2.350	2.350		
exptl[c]	0.210	2.915	2.323	3.250	3.250

[a] The present calculation. [b] From ref 31. [c] From ref 30.

TABLE 2: The B3LYP Optimized Geometry of the Na−NO Complex in Models 2, 3 and 3A

	model 2		model 3		model 3A[a]
geometry	6-31G(d)	6-31+G(d)	6-31G(d)	6-31+G(d)	6-31G(d)
R(N−Na) (Å)	2.695	2.657	2.486	2.490	2.659
R(N−O) (Å)	1.238	1.237	1.225	1.217	1.220
∠ONNa (deg)	129.6	130.7	137.1	138.2	138.1

[a] Na atom of the Na−NO part was relaxed during the optimization.

the experimental value,[30] and is much better than the previously calculated result, 0.74 Å.[31] So, we consider B3LYP to be a reliable method for dealing with this system and that the exchange of two Si atoms for two Al hardly affects the A-zeolite framework.

B. Calculations of NO-Zeolite by Using Model 2. A NO molecule was added to model 2 with the N atom next to the Na atom, which is close to the center of six-membered ring. We kept the framework of model 2, only relaxing the positions of the N and O atoms, and optimized this model at B3LYP/6-31G(d) and B3LYP/6-31+G(d) levels. The bond distance R(N−Na) and bond angle ∠ONNa predicted by B3LYP/6-31G(d) are 2.695 Å and 129.6°, respectively. As seen from Table 2, nearly the same geometry was obtained by the B3LYP/6-31+G(d) calculation on model 2. The calculated isotropic hyperfine coupling a and the principal values B of the dipolar tensor by B3LYP/6-31G(d) and B3LYP/6-31+G(d) are listed in Table 3. The calculated a values for the ^{14}N nucleus agree satisfactorily with the experimental value, and also the dipolar components B for Na and N agree reasonably well with the experimental values. The calculated isotropic couplings for Na are, however, nearly twice that of the experimental value. The calculated bond distance R(N−Na) and bond angle ∠ONNa are also quite different from the experimentally deduced ones,[10] 2.1 Å and 142°, respectively. We tried to use a bigger model, model 3, to solve these problems.

C. Calculations of NO-Zeolite by Using Model 3. A NO molecule was added to model 3 as in model 2. As seen from Table 2, the B3LYP/6-31G(d) and B3LYP/6-31+G(d) optimized bond distance R(N−Na) and bond angle ∠ONNa are 2.486 Å and 137.1°, and 2.490 Å and 138.2°, respectively. The calculated ∠ONNa values are close to 142°, which was predicted by the experiment.[10] However, the bond distances R(N−Na) are still larger than the experimental prediction, 2.11 Å.[10] The experimentally determined anisotropic hyperfine coupling constants were axially symmetric, possibly because of a dynamic averaging between the B_{xx} and B_{yy} components of the ^{14}N tensor, while the computed ^{23}Na tensor was already nearly axial, but an average of the computed anisotropic constants perpendicular to the parallel (z) axis was still considered to be the most reliable for comparison with the ^{23}Na and the ^{14}N experimental values. Except that the a value of Na is obviously larger than the experimental one, the a value of N, and the B tensors of Na and N atoms calculated at both levels agree very well with the experimental values,[10] in both values and directions, see Table 3.

We used the B3LYP/6-31+G(d) optimized geometry to calculate the Q tensors of Na of the Na−NO part and g tensors of the whole complex, see Table 4. Q_{xx}^{Na}, Q_{yy}^{Na}, Q_{zz}^{Na}, and g_{zz} do not agree well with the corresponding experimental values. As noted above, the a value of Na does not agree with the experimental value. To improve the model, we relaxed also the position of the Na atom of the Na−NO part during the geometry optimization. This modification of model 3 with a relaxed Na atom of the six-membered ring is called model 3A. As is seen from Tables 2 and 3, the diffuse basis played very little role in the geometry optimization and a and B calculations for both model 2 and model 3. So, we only used B3LYP/6-31G(d) to totally optimize the Na−NO part in model 3A, cf. Table 2. The R(N−O) and ∠ONNa values changed very slightly compared to the calculated values when Na was fixed. The R(N−Na) value, 2.659 Å, became a little larger, which is farther from the experimental value, 2.11 Å.[10] As described in section IVA, the initial position of the Na atom was 0.21 Å above the six-membered ring. The result of totally optimizing the Na−NO part in model 3A indicated that the Na atom was 0.049 Å below the six-membered ring. The Q tensors of Na of the Na−NO part and g tensors of the whole complex were calculated at this geometry (see Table 4). The calculated a value of Na is 7.3 MHz, which agrees very well with the experimental value of 7.8 MHz. At the same time, the calculated a value of N, and the B tensors of Na and N atoms also agree with the experimental values very well. The calculated Q_{xx}^{Na}, Q_{yy}^{Na}, and Q_{zz}^{Na} values are −0.38, −0.19, and 0.57 MHz, respectively, in close agreement with their corresponding experimental values −0.41, −0.23, and 0.64 MHz, respectively.[10] One may note that the relative signs of these values were measured in the pulsed ENDOR measurements, while the absolute signs can usually not be obtained experimentally. Comparison with the computed values indicates that the absolute signs of the principal components were also correctly assigned. The calculated g_{xx}, g_{yy}, and g_{zz} are 2.030, 1.999, and 1.888, respectively, and their corresponding experimental values are 2.001, 1.996, and 1.888, respectively.[10] The results are summarized in Table 4.

TABLE 3: The B3LYP Calculated Isotropic (a) and Anisotropic (B) Hyperfine Coupling Constants (MHz) of Na and N Atoms of the Na−NO Part in Models 2, 3, and 3A

	model 2		model 3		model 3A[a]	
	6-31G(d)	6-31+G(d)	6-31G(d)	6-31+G(d)	6-31G(d)	exptl[b]
a^{Na}	14.3	16.2	13.3	13.0	7.3	7.8
$(B_{xx}^{Na} + B_{yy}^{Na})/2$	−2.63	−2.70	−2.93	−2.75	−2.14	−1.55
B_{zz}^{Na}	5.26	5.43	5.85	5.49	4.26	3.10
a^{N}	42.3	43.6	39.7	38.4	38.6	47.7
B_{yy}^{N}	39.3	39.7	41.0	42.5	43.4	43.8
$(B_{xx}^{N} + B_{zz}^{N})/2$	−19.7	−19.9	−20.5	−21.2	−21.7	−21.9

[a] Na atom of the Na−NO part was relaxed during the optimization. [b] From ref 10. The computed principal axes of the axially symmetric anisotropic hyperfine coupling constants agreed with those experimentally obtained and are not given here.

TABLE 4: The DFT Calculated *Q* Tensors of the Na Atom of the Na−NO Part in Models 3 and 3A and the *g* Tensors of Models 3 and 3A[a]

	model 3	model 3A[b]	exptl[c]
Q_{xx}^{Na}	−0.23	−0.38	−0.41
Q_{yy}^{Na}	−0.12	−0.19	−0.23
Q_{zz}^{Na}	0.35	0.57	0.64
g_{xx}	2.008	2.030	2.001
g_{yy}	2.003	1.999	1.996
g_{zz}	1.934	1.888	1.888

[a] Quadrupolar coupling principal values are in MHz. [b] Na atom of the Na−NO part was relaxed during the optimization. [c] From ref 10. The relative signs were determined from pulsed ENDOR measurements.

In view of the excellent agreement between calculated and experimental hyperfine parameters, as described above, the big difference in the bond distance R(N−Na) between the calculated and experimentally predicted value is somewhat puzzling. As a test, we used the experimentally predicted geometry of the Na−NO part,[10] R(Na−X) = 0.21 Å, R(N−Na) = 2.11 Å, and bond angle ∠ONNa = 142°, and kept the other parts of model 3 as in the experimental geometry, then did a single point calculation by the B3LYP/6-31G(d) method. The calculated EPR properties are very far from the experimental values, the *a* values of Na and N are 25.4 and 32.94 MHz, respectively. Moreover, it can be noted that a previous DFT calculation[31] on N_2-zeolite also gave a long bond distance R(N−Na) = 2.60 Å. Pöppl et al.[10] deduced the bond distance R(N−Na) = 2.11 Å by using the principal values of the Na dipolar hyperfine coupling tensor and the orientations of the corresponding principal axes with respect to the coordinate frame of the *g* tensors. This distance was thus not directly measured, but depended, e.g., on an assumed distribution of the spin density in the Na^+−NO adsorption complex shown in Figure 1. Thus some uncertainty prevails in the obtained distance and angle, which could at least in part explain the above-mentioned discrepancy.

V. Conclusions

Density functional theory was employed to model the adsorption site of nitric oxide adsorbed in Na-LTA-zeolite using three different models of the zeolite network: (1) a six-membered ring terminated by hydrogen atoms with one sodium ion above the ring, (2) as in model 1, with the addition of three sodium ions located at the centers of the 3 four-membered rings adjacent to the six-membered rings, and (3) as in model 2 with the addition of 3 four-membered rings adjacent to the six-membered ring. Charge neutrality was achieved in all models by an appropriate adjustment of the silicon-to-aluminum ratio in the ring. Calculations on model 1 showed that the Si/Al exchange did not seriously alter the geometry from that of the experimentally determined zeolite structure. Calculations on the bigger models showed very good agreement between measured and calculated electronic *g* and ^{14}N hyperfine coupling tensors, and the ^{23}Na hyperfine and *Q* tensors of the $S = {}^1/_2$ $Na^+\cdots$N−O adsorption complex could be achieved when the position of the sodium ion was relaxed in model 3. The optimized geometry of the complex agreed with that estimated experimentally except for the Na···N distance, which is noticeably longer than the experimentally predicted one. The successful modeling of the NO radical interaction with the zeolite framework opens up possibilities for further theoretical studies in the area, including, e.g., NO dimerization and catalytic degradation.

Acknowledgment. We are indebted to Prof. H. Yahiro, Ehime University, Matsuyama, Japan for valuable discussion. The Swedish Research Council (VR), the Göran Gustafsson Foundation, the Trygger Foundation, and the Magnus Bergvall Foundation are gratefully acknowledged for financial support. The Swedish National Supercomputer Centre (NSC) is acknowledged for generous grants of computer resources.

References and Notes

(1) Iwamoto, M.; Yahiro, H. *Catal. Today* **1994**, *22*, 5.
(2) Yahiro, H.; Iwamoto, M. *Appl. Catal. A* **2001**, *222*, 163.
(3) Lunsford, J. H. *J. Phys. Chem.* **1968**, *72*, 4163.
(4) Gardner, C. L.; Weinberger, M. A. *Can. J. Chem.* **1970**, *48*, 1317.
(5) Kasai, P. H.; Bishop, R. J. B., Jr. *J. Am. Chem. Soc.* **1972**, *94*, 5560.
(6) Kasai, P. H.; Bishop, R. J. B., Jr. In *Zeolite Chemistry and Catalysis*; Rabo, J. A., Ed.; ACS Monograph No. 171; American Chemical Society: Washington, DC, 1976; p 350.
(7) Che, M.; Giamello, E. *Stud. Surf. Sci. Catal.* **1990**, *57*, B265.
(8) Rudolf, T.; Pöppl, A.; Brunner, W.; Michel, D. *Magn. Reson. Chem.* **1999**, *77*, 93.
(9) Rudolf, T.; Pöppl, A.; Hofbauer, W.; Michel, D. *Phys. Chem. Chem. Phys.* **2001**, *3*, 2167.
(10) Pöppl, A.; Rudolf, T.; Manikandan, P.; Goldfarb, D. *J. Am. Chem. Soc.* **2000**, *122*, 10194.
(11) Rudolf, T.; Böhlmann, W.; Pöppl, A. *J. Magn. Reson.* **2002**, *155*, 45.
(12) Pietrzyk, P.; Piskorz, W.; Sojka, Z.; Broclawik, E. *J. Phys. Chem. B* **2003**, *107*, 6105.
(13) Freysoldt, C.; Pöppl, A.; Reinhold, J. *J. Phys. Chem. A* **2004**, *108*, 1582.
(14) Davidová, M.; Nachtgallová, D.; Nachtigall, P.; Sauer, J. *J. Phys. Chem. B* **2004**, *108*, 13674.
(15) Hohenberg, P.; Kohn, W. *Phys. Rev. B* **1964**, *136*, 864.
(16) Kohn, W.; Sham, L. J. *Phys. Rev. A* **1965**, *140*, 1133.
(17) Biglino, D.; Li, H.; Erickson, R.; Lund, A.; Yahiro, H.; Shiotani, M. *Phys. Chem. Chem. Phys.* **1999**, *1*, 2887.
(18) Biglino, D.; Bonora, M.; Volodin, A.; Lund, A. *Chem. Phys. Lett.* **2001**, *349*, 511.
(19) Becke, A. D. *J. Chem. Phys.* **1993**, *98*, 5648.
(20) Lee, C.; Yang, W.; Parr, R. G. *Phys. Rev. B* **1988**, *37*, 785.
(21) Frisch, M. J.; Trucks, G. W.; Schlegel, H. B.; Scuseria, G. E.; Robb, M. A.; Cheeseman, J. R.; Montgomery, J. A., Jr.; Vreven, T.; Kudin, K. N.; Burant, J. C.; Millam, J. M.; Iyengar, S. S.; Tomasi, J.; Barone, V.; Mennucci, B.; Cossi, M.; Scalmani, G.; Rega, N.; Petersson, G. A.; Nakatsuji, H.; Hada, M.; Ehara, M.; Toyota, K.; Fukuda, R.; Hasegawa, J.; Ishida, M.; Nakajima, T.; Honda, Y.; Kitao, O.; Nakai, H.; Klene, M.; Li, X.; Knox, J. E.; Hratchian, H. P.; Cross, J. B.; Adamo, C.; Jaramillo, J.; Gomperts, R.; Stratmann, R. E.; Yazyev, O.; Austin, A. J.; Cammi, R.; Pomelli, C.; Ochterski, J. W.; Ayala, P. Y.; Morokuma, K.; Voth, G. A.; Salvador, P.; Dannenberg, J. J.; Zakrzewski, V. G.; Dapprich, S.; Daniels, A. D.; Strain, M. C.; Farkas, O.; Malick, D. K.; Rabuck, A. D.; Raghavachari, K.; Foresman, J. B.; Ortiz, J. V.; Cui, Q.; Baboul, A. G.; Clifford, S.; Cioslowski, J.; Stefanov, B. B.; Liu, G.; Liashenko, A.; Piskorz, P.; Komaromi, I.; Martin, R. L.; Fox, D. J.; Keith, T.; Al-Laham, M. A.; Peng, C. Y.; Nanayakkara, A.; Challacombe, M.; Gill, P. M. W.; Johnson, B.; Chen, W.; Wong, M. W.; Gonzalez, C.; Pople, J. A. *Gaussian 03*, Revision A.1; Gaussian, Inc: Pittsburgh, PA, 2003.
(22) Ditchfield, R.; Hehre, W. J.; Pople, J. A. *J. Chem. Phys.* **1971**, *54*, 724.
(23) Petersson, G. A.; Bennett, A.; Tensfeldt, T. G.; Al-Laham, M. A.; Shirley, W. A.; Mantzaris, J. *J. Chem. Phys.* **1988**, *89*, 2193.
(24) Boese, A. D.; Handy, N. C. *J. Chem. Phys.* **2001**, *114*, 5497.
(25) Becke, A. D. *Phys. Rev. A* **1988**, *38*, 3098.
(26) Perdew, J. P. *Phys. Rev. B* **1986**, *33*, 8822.
(27) Schaefer, A.; Horn, H.; Ahlrichs, R. *J. Chem. Phys.* **1992**, *97*, 2571.
(28) Lenthe, E. v.; Snijders, J. G.; Baerends, E. J. *J. Chem. Phys.* **1996**, *105*, 6505.
(29) Scientific Computing and Modeling, T. C. Amsterdam Density Functional (ADF) version 2002.03; Vrije Universiteit: Amsterdam, The Netherlands, 2002.
(30) Pluth, J. J.; Smith, J. V. *J. Am. Chem. Soc.* **1980**, *102*, 4704.
(31) Papai, I.; Goursot, A.; Fajula, F.; Plee, D.; Weber, J. *J. Phys. Chem.* **1995**, *99*, 12925.